



## ORIGINAL ARTICLE

# *Verbascum chinense* L. leaf aqueous extract green-synthesized nanoparticles: Its performance in the treatment of several types of human lung cancers



Yuqiong Fu <sup>a,1</sup>, Ping Wang <sup>b,1</sup>, Wei Zhou <sup>c</sup>, Long Lv <sup>d</sup>, Yihui Fan <sup>e,\*</sup>,  
Tahani Awad Alahmadi <sup>f</sup>, Sulaiman Ali Alharbi <sup>g</sup>, Milton Wainwright <sup>h</sup>

<sup>a</sup> Department of Respiratory and Critical Care Medicine, The Affiliated Hospital of Southwest Medical University, Luzhou, Sichuan 646000, China

<sup>b</sup> Department of Internal Medicine, Nanjing Gaochun People's Hospital, Jiangsu Province, Nanjing, Jiangsu 211300, China

<sup>c</sup> Department of Neurosurgery, The Affiliated Traditional Chinese Medicine Hospital of Southwest Medical University, Luzhou 646000, China

<sup>d</sup> Department of General Surgery, Nanjing Gaochun People's Hospital, Nanjing, Jiangsu 211300, China

<sup>e</sup> Department of Thoracic Surgery, Tumor Hospital Affiliated To Nantong University (Thoracic Surgery, Nantong Tumor Hospital), Nantong, Jiangsu 226361, China

<sup>f</sup> Department of Pediatrics, College of Medicine and King Khalid University Hospital, King Saud University, Medical City, PO Box-2925, Riyadh 11461, Saudi Arabia

<sup>g</sup> Department of Botany and Microbiology, College of Science, King Saud University, PO Box -2455, Riyadh 11451, Saudi Arabia

<sup>h</sup> Department of Molecular Biology and Biotechnology, University of Sheffield, Sheffield S10 2TN, UK

Received 13 July 2021; revised 25 August 2021; accepted 26 August 2021

Available online 1 September 2021

## KEYWORDS

Gold nanoparticles;  
*Verbascum chinense* L.;  
Lung well-differentiated  
bronchogenic adenocarci-  
noma;  
Lung moderately differenti-

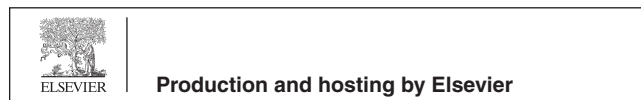
**Abstract** In recent years, scientists have tried to increase organic chemistry productions for the treatment of many cancers such as the lung cancers. In this regard, gold nanoparticles have a special place. Furthermore, one of the therapeutic properties of *Verbascum chinense* L. is increasing the physiological potentials of the body against several cancers. In the present study, gold nanoparticles were prepared and synthesized in aqueous medium using *V. chinense* leaf extract. We assessed the anti-human lung cancers potentials of these nanoparticles against well-differentiated bronchogenic adenocarcinoma, moderately differentiated adenocarcinoma of the lung, and poorly differentiated

\* Corresponding author.

E-mail address: [fanyihui1987@sina.com](mailto:fanyihui1987@sina.com) (Y. Fan).

<sup>1</sup> means Yuqiong Fu and Ping Wang contributed equally to the article.

Peer review under responsibility of King Saud University.



ated adenocarcinoma;  
Lung poorly differentiated  
adenocarcinoma

adenocarcinoma of the lung cell lines. AuNPs were characterized and analyzed by common nanotechnology techniques including FT-IR and UV-Vis. Spectroscopy, Field Emission-Scanning Electron Microscopy, and Transmission Electron Microscopy. In the FT-IR test, the presence of many antioxidant compounds with related bonds caused the excellent condition for reducing of gold in the gold nanoparticles. In UV-Vis, the clear peak in the wavelength of 542 nm indicated the formation of gold nanoparticles. We assessed the anti-human lung cancers potentials of these nanoparticles against well-differentiated bronchogenic adenocarcinoma, moderately differentiated adenocarcinoma of the lung, and poorly differentiated adenocarcinoma of the lung cell lines. AuNPs had excellent anti-human lung cancer effects dose-dependently against HLC-1, LC-2/ad, and PC-14 cell lines. The best result of anti-human lung cancer activities of AuNPs against above cell lines was observed in the case of the PC-14 cell line. In conclusion, the synthesized AuNPs showed significant anti-human lung cancer properties against well-differentiated bronchogenic adenocarcinoma, moderately differentiated adenocarcinoma of the lung, and poorly differentiated adenocarcinoma of the lung cell lines in a dose depended on manner. After confirming in the *in vivo* and clinical trials, AuNPs can be administrated in human for the treatment of humans' lung cancers especially well-differentiated bronchogenic adenocarcinoma, moderately differentiated adenocarcinoma of the lung, and poorly differentiated adenocarcinoma of the lung.

© 2021 Published by Elsevier B.V. on behalf of King Saud University. This is an open access article under the CC BY-NC-ND license (<http://creativecommons.org/licenses/by-nc-nd/4.0/>).

## 1. Introduction

Lung is the last part of the respiratory tract that participates in the transferring of respiratory gases such as O<sub>2</sub> and CO<sub>2</sub>. The normal function of the lung is necessary for the routine activities of the body (Cancer Research UK [cruk.org/cancerstats](http://cruk.org/cancerstats), 2013). The main diseases that affect the normal function of the lung are included cold, flu, and cough, tuberous sclerosis, cystic fibrosis, chronic obstructive pulmonary disease, allergies, asthma, bronchitis, pulmonary hypertension, tuberculosis, pneumonia, emphysema, and lung cancer. Among the above diseases, the mortality rate of lung cancer is more (Cancer Research UK [cruk.org/cancerstats](http://cruk.org/cancerstats), 2013; Jemal et al., 2011). Lung cancer is the most common cancers in men, also one of the most common cancers in the woman. The common signs of lung cancer are weakness, weight loss, hoarseness, fatigue, coughing up blood, wheezing, cough, shoulder pain, shortness of breath, chest pain, and dysphagia. The symptoms of the metastasis of lung cancer are symptoms of stroke such as weakness, headaches, seizures, and blurred vision (Cancer Research UK [cruk.org/cancerstats](http://cruk.org/cancerstats), 2013; Centers for Disease Control and Prevention (US), 2004). The main risk factors of lung cancer are radiation therapy, smoking, exposure to asbestos fibers, exposure to radon gas, exposure to diesel exhaust, air pollution, and familial predisposition (Centers for Disease Control and Prevention (US), 2004). The history and physical examination, sputum cytology, bronchoscopy, needle biopsy, thoracentesis, blood tests, molecular testing, and medical imaging such as chest X-ray, computerized tomography, low-dose helical computerized tomography scan, magnetic resonance imaging, and positron emission tomography are used for diagnosis of lung cancer (Rodriguez and Lilenbaum, 2010). For the treatment of lung cancer, surgery, chemotherapy, radiation therapy, targeted therapy, immunotherapy, and EGFR-targeted therapy are used. The main anti-lung cancer chemotherapeutic drugs are included ceritinib (Zykadia), alectinib (Alecensa), brigatinib (Alunbrig), and crizotinib (Xalkori) (Chemotherapy, 2011). According to the high side effects of chemotherapeutic

drugs such as weight loss, mouth sores, vomiting, diarrhea, hair loss, fatigue, and nausea, the formulation of modern chemotherapeutic drugs is necessary (Chemotherapy, 2011). From past to now, scientists have understood that metallic nanoparticles have excellent anticancer properties (Zangeneh and Zangeneh, 2019; Hemmati et al., 2019).

Recently, the metal-based nanoparticles with distinctive physicochemical properties have been considered as a promising alternative medicine for the treatment of several diseases (Ball, 2018). In earlier times, gold was used as a therapeutic agent. Nanoparticles are widely used because of their high surface-to-volume ratio, small size, and excellent reactivity. One of the most important advances in nanotechnology is the production and application of nanoparticles in the biological sciences (Chemotherapy, 2011; Zangeneh and Zangeneh, 2019; Hemmati et al., 2019). Nanoparticles are generally effective in a wide variety of sectors that if their production is based on green chemistry, they have great applications in the fields of food, medicine, cosmetics and health. Nanoparticles centered on inorganic materials such as magnetic metals, their oxides and alloys, and semiconductors have the most studies and potential in biomedicine from diagnosis to treatment of diseases (Hemmati et al., 2019; Ball, 2018; Sintubin et al., 2009). Metallic nanoparticles used in treatment and diagnosis, in addition to being non-toxic, must be biocompatible and stable *in vivo*. Also, by making appropriate changes in the surface of metallic nanoparticles, they will have a wide range of applications by binding to biomolecules and various carriers to cross the cell membrane and target the desired part in the body (Arunachalam et al., 2003; Varma, 2012; Raut et al., 2010).

There are three biological, chemical, and physical methods to synthesize the nanoparticles. Chemical and physical methods are time-consuming and costly. In addition, these methods use some toxic additive chemicals that cause adverse effects on medical applications by adsorption on the surface. Applying the principles of green chemistry has decreased the use of toxic compounds or hazardous solvents, provided optimal regeneration conditions and ameliorated materials for the chemical

processes, and raised new sources for green synthesis (Zangeneh et al., 2019; Zangeneh et al., 2019; Zangeneh et al., 2019; Zangeneh et al., 2019). Therefore, one of the primary goals of green nanotechnology is to produce nanomaterials without harm to human health or environment, and to develop and design nanomaterials and products that are suitable solutions to environmental problems. The synthesis of nanoparticles by similar biological methods results in greater catalytic activity and limits the use of toxic and expensive chemicals. In biological methods, plant extracts, enzymes or proteins carrying natural resources are used to produce or stabilize nanoparticles. The nature of the materials used to make nanoparticles influences the shape, structure and morphology of these nanoparticles (Zangeneh et al., 2019; Tveden-Nyborg et al., 2018; Riaza et al., 2013). Biological systems involved in the green synthesis of nanoparticles, plants and their derivatives, as well as microorganisms such as algae, fungi, and bacteria. Plant parts such as roots, leaves, stems, fruits, and tiny parts such as the kernel and skin of the fruit are suitable to synthesize the nanoparticles because their extracts are rich in phytochemicals that act as stabilizing and reducing substances (Zangeneh and Zangeneh, 2019; Ball, 2018). The use of natural plant extracts is a cheap and environmentally friendly process and does not require intermediate groups. Short time, no need for expensive equipment, precursors, high purity product and excellent quality without impurities are the features of this method. This is possible very quickly, at room temperature and pressure as well as easily on a large scale. Bio-reduction in the conversion of base metal ions is carried out by various plant metabolites such as alkaloids, phenolic compounds, terpenoids and coenzymes (Shahriari et al., 2019; Soni and Krishnamurthy, 2013). Recently, scientists have used the anticancer effects of medicinal plants in several traditional medicines for synthesizing the gold nanoparticles containing natural compounds. So far, the anticancer effects of *Tinospora cordifolia*, *Sophora subprostrata*, *Euphoria hirta*, *Barleria prionitis*, *Lubinus perennis*, *Maytenus boaria*, *Cephaelis acuminata*, *Phyllanthus niruri*, *Solanum seafortianum*, *Boswellia serrate*, *Lavendula officinalis*, and *Cephalotaxus harringtonia* drupacea have been proved (Soni and Krishnamurthy, 2013).

One of these plants is *Verbascum chinense* L. The genus *Verbascum* L. (Scrophulariaceae) is a widespread genus of the family Scrophulariaceae. The genus is represented by 233 species, 196 of which are endemic in Turkish Flora. Many internal and external uses of the leaves and flowers of several *Verbascum* L. species have been documented in many societies in Europe, Asia, Africa, and North America. These species have been used in traditional folk medicine for centuries, for treatment of a wide range of human ailments, inter alia bronchitis, tuberculosis, asthma, and different inflammations (Peng et al., 2009). It has chemical antioxidant components including  $\beta$ -carotene, lutein, zeaxanthin, cryptoxanthin, triterpene A, triterpene B, saikogenin A, veratric acid,  $\beta$ -spinasterol, 6-*O*- $\beta$ -*D*-xylopyranosyl aucubin, thapsuine B, hydroxythapsuine thapsuine A, 3-*O*-fucopyranosylsaikogenin F,  $\alpha$ -tocopherol,  $\gamma$ -tocopherol, and  $\delta$ -tocopherol (Peng et al., 2009). Probably, the remedial properties of this genus are related to the above compounds.

In the recent research, we decided to investigate the anti-human lung cancer effects of gold nanoparticles formulated by *Verbascum chinense* against well-differentiated bron-

chogenic adenocarcinoma, moderately differentiated adenocarcinoma of the lung, and poorly differentiated adenocarcinoma of the lung cell lines.

## 2. Experimental

### 2.1. Material

Antimycotic antibiotic solution, decamplmaneh fetal bovine serum, Dulbecco's Modified Eagle Medium (DMEM), carbazole reagent, 2,2-diphenyl-1-picrylhydrazyl (DPPH), 4-(Dimethylamino)benzaldehyde, phosphate buffer solution (PBS), borax-sulphuric acid mixture, Ehrlich solution, hydrolysate, and dimethyl sulfoxide (DMSO), all were achieved from Sigma-Aldrich company of USA.

### 2.2. Synthesis of AuNPs

Extraction was carried out by dissolving 100 g of *Verbascum chinense* leaf powder in 1000 mL of distilled water and kept on an orbital shaker for 48 h. Then the extract was filtered using Whatman filter paper No. 1 and the filtrate was concentrated in a rotary evaporator under reduced pressure ( $60 \pm 100$  C). Furthermore, the herbal extracts were lyophilized at  $-48$  °C for 24 h and stored for further use (Zangeneh and Zangeneh, 2019; Hemmati et al., 2019).

The green synthesis of the AuNPs was initiated with a reaction mixture of 100 mL of  $\text{HAuCl}_4 \cdot \text{H}_2\text{O}$  in the concentration of  $1 \times 10^{-3}$  M and 200 mL of aqueous extract solution of *Verbascum chinense* leaf (20  $\mu\text{g}/\text{mL}$ ) in the proportion 1:10 in a conical flask (Fig. 1). The reaction mixture was kept under magnetic stirring for 12 h at room temperature. At the end of the reaction time, the dark red colored colloidal solution of Au was formed. The mixture was centrifuged at 10000 rpm for 15 min. The precipitate was triplet washed with water and centrifuged subsequently (Zangeneh and Zangeneh, 2019; Hemmati et al., 2019). For analyzing AuNPs, the common techniques of organic chemistry, i.e. FT-IR and UV-Vis. spectroscopy, FE-SEM, and TEM were used. AuNPs were primarily confirmed using UV-Vis spectroscopy at a scan range from 450 to 750 nm wavelength (Jasco V670 Spectrophotometer). The biomolecules involved in the reduction of AuNPs were detected by the FT-IR spectrophotometer (Shimadzu IR affinity.1). The morphological features in terms of shape and sizes were analyzed by FE-SEM (Fe-SEM ZEISS EVO18) and TEM (TEM FEI-TECNAI G2-20 TWIN) microscopic techniques.

### 2.3. Assessment of the antioxidant potential of AuNPs by DPPH

Free radicals are unstable atoms that have one or more unpaired electrons. These active species are very harmful due to their high reactivity. They are most often formed when oxygen molecules in the body split into separate unstable atoms. This process can turn into a chain reaction. Free radicals' excessive production in the body causes cell damage and oxidative stress. Genetics and the environment affect the extent of free radical damage in individuals. These active molecules are produced as part of the body's natural biological processes. One of the most important free radicals is DPPH. DPPH is

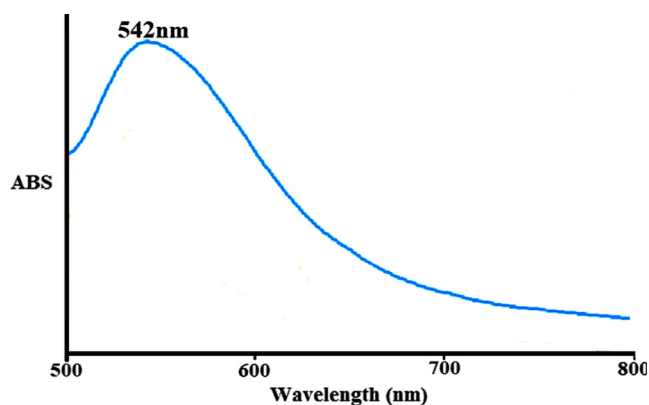


**Fig. 1** The UV-Vis spectrum of biosynthesized gold nanoparticles.

widely used to study the antioxidant activities of natural compounds and nanoparticles (Singh et al., 1979; Hosseinimehr et al., 2011).

At the beginning of the study, 100 mL of methanol (50 %) was added to the 39.4 g of DPPH. Also, several concentrations of  $\text{HAuCl}_4$ , *Verbascum chinense*, and AuNPs i.e., 0–1000  $\mu\text{g/mL}$  were considered. The above DPPH was added to the various concentrations of  $\text{HAuCl}_4$ , *Verbascum chinense*, and AuNPs and all samples were transfer to an incubator at the temperature of 37 °C. After 30 min incubating, the absorbances were measured at 517 nm. In this study, methanol (50 %) and butylated hydroxytoluene (BHT) were negative and positive controls, respectively. According to the following formula, the antioxidant properties of  $\text{HAuCl}_4$ , *Verbascum chinense*, and AuNPs were determined (Singh et al., 1979; Hosseinimehr et al., 2011):

$$\text{DPPH free radical scavenging (\%)} = \left( \frac{\text{Control} - \text{Test}}{\text{Control}} \right) \times 100$$

#### 2.4. Measurement of cell toxicity of AuNPs

MTT method (3-(4,5-dimethylthiazol-2-yl)-2,5-diphenyltetrazolium bromide) is a colorimetric method to study cell proliferation and survival, introduced in 1983 by Mossman. The method basis is based on mitochondrial activity. Mitochondrial activity in living cells is stable and therefore a raise or reduce in the living cells number is linearly related to mitochondrial activity. <sup>[23]</sup> MTT tetrazolium dye is revived in active cells. Mitochondrial dehydrogenases in living cells break the tetrazolium ring and yield NADPH and NADH, leading to forming a purple insoluble deposit called formazan. This precipitate can be dissolved by dimethyl sulfoxide or isopropanol. On the other hand, dead cells do not have this ability and therefore do not reveal a signal. Dye formation is used as a marker of living cells. The color intensity produced is measured at a 540 to 630 nm wavelength and is directly proportional to the living cells number. High safety and providing a colorimetric and non-radioactive system are important advantages of this method. This kit is very easy to use, has high sensitivity and accuracy and can detect less than 950 cells. On the other hand, it has high efficiency for measuring cell proliferation, survival and mortality, and its implementation method

does not require time-consuming washing steps and transfer from one plate to another. Examples studied in this method are adhesive or suspended cells and proliferating or non-proliferating cells (Arulmozhi et al., 2013).

In this experiment, the following cell lines have been used for investing the cytotoxicity and anti-human lung cancer effects of the  $\text{HAuCl}_4$ , *Verbascum chinense*, and AuNPs using an MTT assay:

- 1) Normal cell line: HUVEC.
- 2) Well-differentiated bronchogenic adenocarcinoma cell line: HLC-1.
- 3) Moderately differentiated adenocarcinoma of the lung cell line: LC-2/ad.
- 4) Poorly differentiated adenocarcinoma of the lung cell line: PC-14.

For culturing the above cells, penicillin, streptomycin, and Dulbecco's modified Eagle's medium (DMEM) were used. The distribution of cells was 10,000 cells/well in 96-well plates. Then, all samples were transferred to a humidified incubator with 5%  $\text{CO}_2$  at the temperature of 37 °C. After 24 h incubating, all cells were treated with several concentrations of  $\text{HAuCl}_4$ , *Verbascum chinense*, and AuNPs, then incubated for 24 h.  $\text{HAuCl}_4$ , *Verbascum chinense*, and AuNPs were sterilized using the radiation of UV for 2 h. Finally, 5 mg/mL of MTT was added to all wells and all samples were transfer to an incubator at the temperature of 37 °C for 4 h. The percentage of cell viability of samples was measured at the absorbance of 570 nm and according to the following formula (Arulmozhi et al., 2013):

$$\text{Percentage of cell viability (\%)} = \left( \frac{\text{Sample absorbance}}{\text{Control absorbance}} \right) \times 100$$

Finally, linear regression was done to gain  $\text{IC}_{50}$ , which indicates the nanoparticles concentration, which causes 50% cancer cell growth inhibition. Using the curve, the line equation for cancer cells was obtained, respectively, then by replacing 50% inhibition in the equation, the  $\text{IC}_{50}$  value for cancer cells was obtained (Arulmozhi et al., 2013).

#### 2.5. Statistical analysis

The obtained results were fed into SPSS-22 software and analyzed by one-way ANOVA, followed by Duncan post-hoc test ( $p \leq 0.01$ ).

### 3. Results and discussion

From past decades, gold nanoparticles paid continuous attention by the research community due to their size and morphology dependent properties as compared from their bulk counterparts (Mehwish et al., 2019; Kumar et al., 2017). Hence, the synthesis of gold nanoparticles was now being increased owing to their wide range of applications, including electronics, environmental remediation, uses in medicine, clothing, renewable energy, engineering, pesticide and fertilizer applications (Jin et al., 2019; van der Heijden, 2018). A variety of physical and chemical routes were employed to prepare gold nanoparticles, which need high temperatures, sophisticated instruments and chemical additives (Shah et al., 2008;

Deshmukh et al., 2019). Present trends in chemical routes to synthesis gold nanoparticles have increased environmental issues due to the use of toxic reagents. Hence, the use of biogenic sources, namely algae, plants and microorganisms for the synthesis of gold nanoparticles was much exciting in the research community. Among, various plant extracts were commonly used as the starting material for the preparation of gold nanoparticles to avoid the production of toxic components. Particularly medicinal plant extracts were used as an antibacterial, antioxidant and anticancer agents (Pereira et al., 2012). According to the above explanations, we tried to prepare and formulate gold nanoparticles in aqueous medium using *V. chinense* leaf aqueous extract as a modern chemotherapeutic drug for the treatment of several types of human lung cancer including well-differentiated bronchogenic adenocarcinoma, moderately differentiated adenocarcinoma of the lung, and poorly differentiated adenocarcinoma of the lung.

### 3.1. UV-visible spectroscopy of gold nanoparticles synthesized using *Verbascum chinense*

UV-Vis spectroscopic analysis showed the presence of an absorption peak at 542 nm which confirmed the formation of the gold nanoparticles (Fig. 1).

In agreement with our study, Shahriari et al. (Shahriari et al., 2019) reported *Allium noeanum* Reut. ex Regel aqueous extract synthesized gold nanoparticles with a peak at 542 nm in the UV-Visible spectrum (Shahriari et al., 2019). Zhaleh et al. (Zhaleh et al., 2019) reported the absorbance at 528 nm for gold nanoparticles synthesized by *Gundelia tournefortii* L. (Zhaleh et al., 2019). Zangneh et al. (2019) studied *Falcaria vulgaris* aqueous extracts mediated synthesis of gold nanoparticles. Absorption in the spectrum was noted in the wavelength of 535 nm (Zangeneh and Zangeneh, 2019). Hemmati et al. (Hemmati et al., 2019) reported *Thymus vulgaris* leaf aqueous extract mediated gold nanoparticles and absorption peak was observed at 532 nm (Hemmati et al., 2019).

These reports support the results of the current work.

### 3.2. TEM analysis of gold nanoparticles synthesized using *Verbascum chinense*

TEM is the other test for determining the morphology and size of metallic nanoparticles. In our study, the range size of the nanoparticles (10–31 nm) calculated through TEM images (Fig. 2).

Furthermore, the histogram plot from the TEM image showed the particle size distribution of biosynthesized gold nanoparticles ranges of 16 to 22 nm. In the previous studies, the size of gold nanoparticles formulated by aqueous extract of medicinal plants had been calculated in the ranges of 10–45 nm with the shape of spherical (Zangeneh and Zangeneh, 2019; Hemmati et al., 2019; Zhaleh et al., 2019; Shahriari et al., 2019). These reports support the results of the current work.

### 3.3. FT-IR analysis of gold nanoparticles synthesized using *Verbascum chinense*

The FT-IR spectrum of gold nanoparticles is shown in Fig. 3. The formation of gold nanoparticles is approved by the pres-

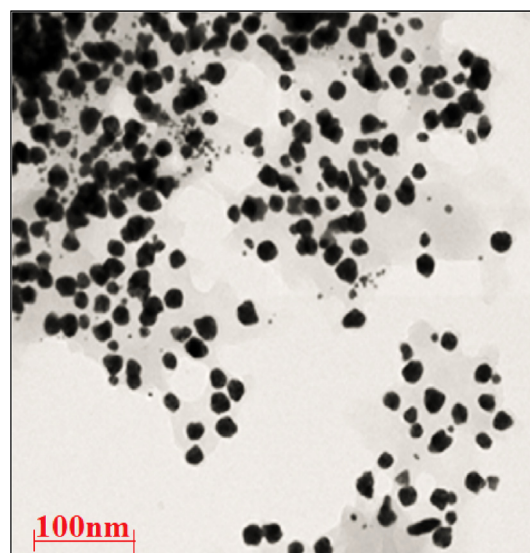


Fig. 2 TEM image of gold nanoparticles.

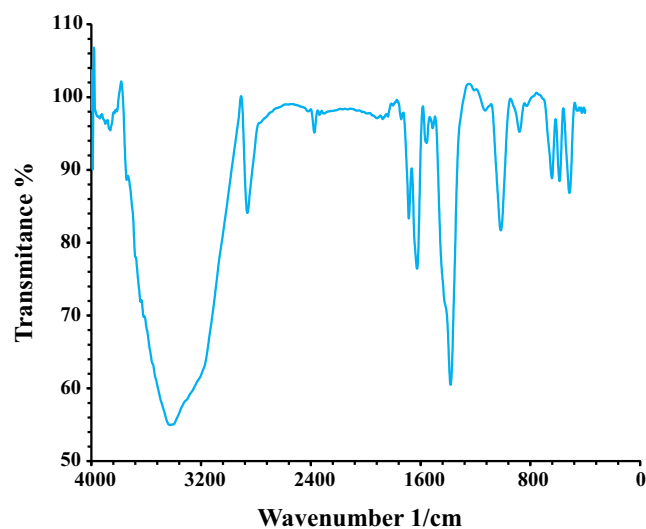


Fig. 3 FT-IR spectra of biosynthesized gold nanoparticles.

ence of the peaks at wavenumbers of 515, 584 and 647  $\text{cm}^{-1}$ . Similar peaks with some differences in the wavenumber have been reported for green-synthetic AgNPs by other research groups (Zhaleh et al., 2019; Shahriari et al., 2019; Zangeneh et al., 2019). The other peaks in the spectrum are attributed to the functional groups of different organic compounds in *Verbascum chinense* extract, which are linked to the surface of gold nanoparticles. The presence of secondary metabolites such as phenolic, flavonoid, saponins, Quinones, Terpenoids in *Verbascum chinense* extract has been reported previously (Peng et al., 2009). The peaks in 3423 and 2921  $\text{cm}^{-1}$  are related to O–H and aliphatic C–H stretching; the peaks from 1550 to 1683  $\text{cm}^{-1}$  are corresponded to C=C and C=O stretching, and the peaks at 1010  $\text{cm}^{-1}$  could be ascribed to C–O and C–O–C stretching (Fig. 3).

### 3.4. FE-SEM analysis of gold nanoparticles synthesized using *Verbascum chinense*

FE-SEM analysis is one of the common chemistry tests for determining the morphology and size of several materials such as metallic nanoparticles.

In the present study, the FE-SEM image of gold nanoparticles synthesized using *Verbascum chinense* leaf aqueous extract is shown in Fig. 4. The gold nanoparticles appeared as an agglomerated structure. The hydroxyl groups present in *Verbascum chinense* could be responsible for agglomeration (Ramyaadevi et al., 2012). Also, FE-SEM images indicated the range size of 7–42 nm and the shape of spherical for gold nanoparticles. Many similar observations are noted by Zhaleh et al. (2019) (Zhaleh et al., 2019), Zangneh et al. (2019) (Zangeneh and Zangeneh, 2019); Hemmati et al. (2019) (Hemmati et al., 2019); and Shahriari et al. (2019) (Shahriari et al., 2019).

### 3.5. Antioxidant properties of gold nanoparticles synthesized using *Verbascum chinense*

Usually, many free radicals such as Reactive oxygen species (ROS) are produced in the procedure of mitochondrial respiration which is responsible for oxidative stress in the human body. This oxidative stress damages human body DNA and develops several oxidative diseases like nephrotoxicity, hepatotoxicity, and hematotoxicity. The oxidative stress can be efficiently reduced with the help of antioxidant materials such as metallic nanoparticles (Gultekin et al., 2016). The synthesized gold nanoparticles exhibit higher antioxidant activity for the formation of free radicals into the living system (Gultekin et al., 2016). The gold nanoparticles have redox properties and play a significant role in deactivating free radicals in the living system (Rehana et al., 2017; Del Mar Delgado-Povedano et al., 2016; Jeong et al., 2012; Sankar et al., 2014). In recent years, researchers evaluated plants and bio mediated synthesized nanoparticles for antioxidant activity. The reason behind the antioxidant activity of green or biosynthesized nanoparticles could be due to the presence of metabolites compounds such as phenolic compounds, flavonoids, carbohydrates, and other sugar substances (Ramyaadevi et al., 2012; Gultekin et al., 2016; Rehana et al., 2017; Del Mar Delgado-Povedano et al., 2016; Jeong et al., 2012; Sankar et al., 2014). Also, many researchers reported phenolic and flavonoids attached to the nanoparticles exhibited the antioxidant activity.

In the present experiment, the antioxidant effects of the gold nanoparticles synthesized using *Verbascum chinense* leaf aqueous extract were evaluated by DPPH assay revealed concentration-dependent effects i.e., an increase in the concentration of the gold nanoparticles leads to an increase in antioxidant activities. In the concentrations of studied, the best result was seen in the high concentration or 1000  $\mu\text{g/mL}$  (Fig. 5).

Comparative analysis of the individual antioxidant assays showed significant variations in the exertion of radical scavenging effects. Among all materials tested (HAuCl<sub>4</sub>, *Verbascum chinense*, and AuNPs), the gold nanoparticles indicated more excellent inhibition effects against DPPH. In contrast,

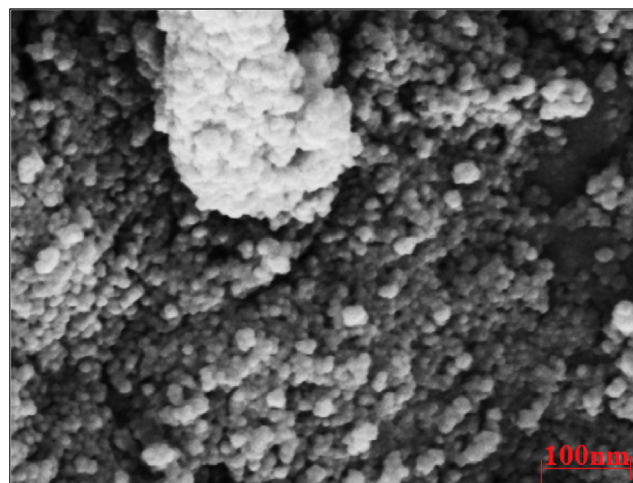


Fig. 4 FE-SEM image of gold nanoparticles.

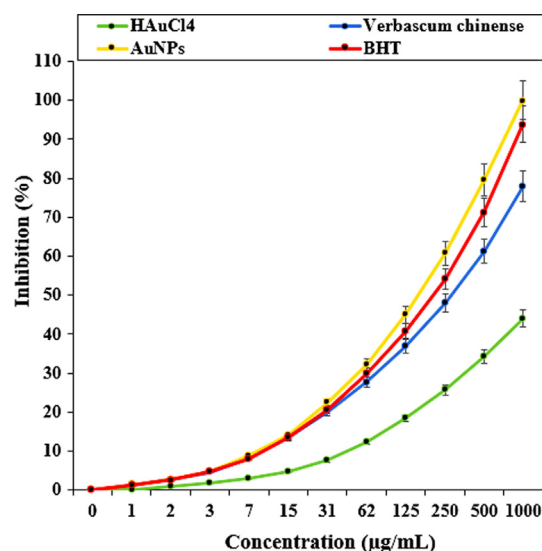


Fig. 5 The antioxidant properties of HAuCl<sub>4</sub>, *Verbascum chinense*, AuNPs, and BHT against DPPH.

standard (butylated hydroxytoluene) demonstrated lower antioxidant effects compared to the gold nanoparticles.

The IC<sub>50</sub> of *Verbascum chinense*, butylated hydroxytoluene, and AuNPs were 269, 163, and 209  $\mu\text{g/mL}$ , respectively (Table 1).

Previously it has been indicated that *Verbascum chinense* is rich in antioxidant compounds such as  $\beta$ -carotene, lutein, zeaxanthin, cryptoxanthin, triterpene A, triterpene B, saikogenin A, veratric acid,  $\beta$ -spinasterol, 6-O- $\beta$ -D-xylopyranosyl aucubin, thapsuine B, hydroxythapsuine thapsuine A, 3-O-fucopyranosylsaikogenin F,  $\alpha$ -tocopherol,  $\gamma$ -tocopherol, and  $\delta$ -tocopherol (Peng et al., 2009). Several studies were carried out in the nanotechnology field using various medicinal plants, but still, no report is available on gold nanoparticles synthesized using *Verbascum chinense* leaf aqueous extract.

**Table 1** The IC<sub>50</sub> of HAuCl<sub>4</sub>, *Verbascum chinense*, AuNPs, and BHT in antioxidant test.

	HAuCl <sub>4</sub> (μg/mL)	<i>Verbascum chinense</i> (μg/mL)	AuNPs (μg/mL)	BHT (μg/mL)
IC <sub>50</sub> against DPPH	–	269	163	209

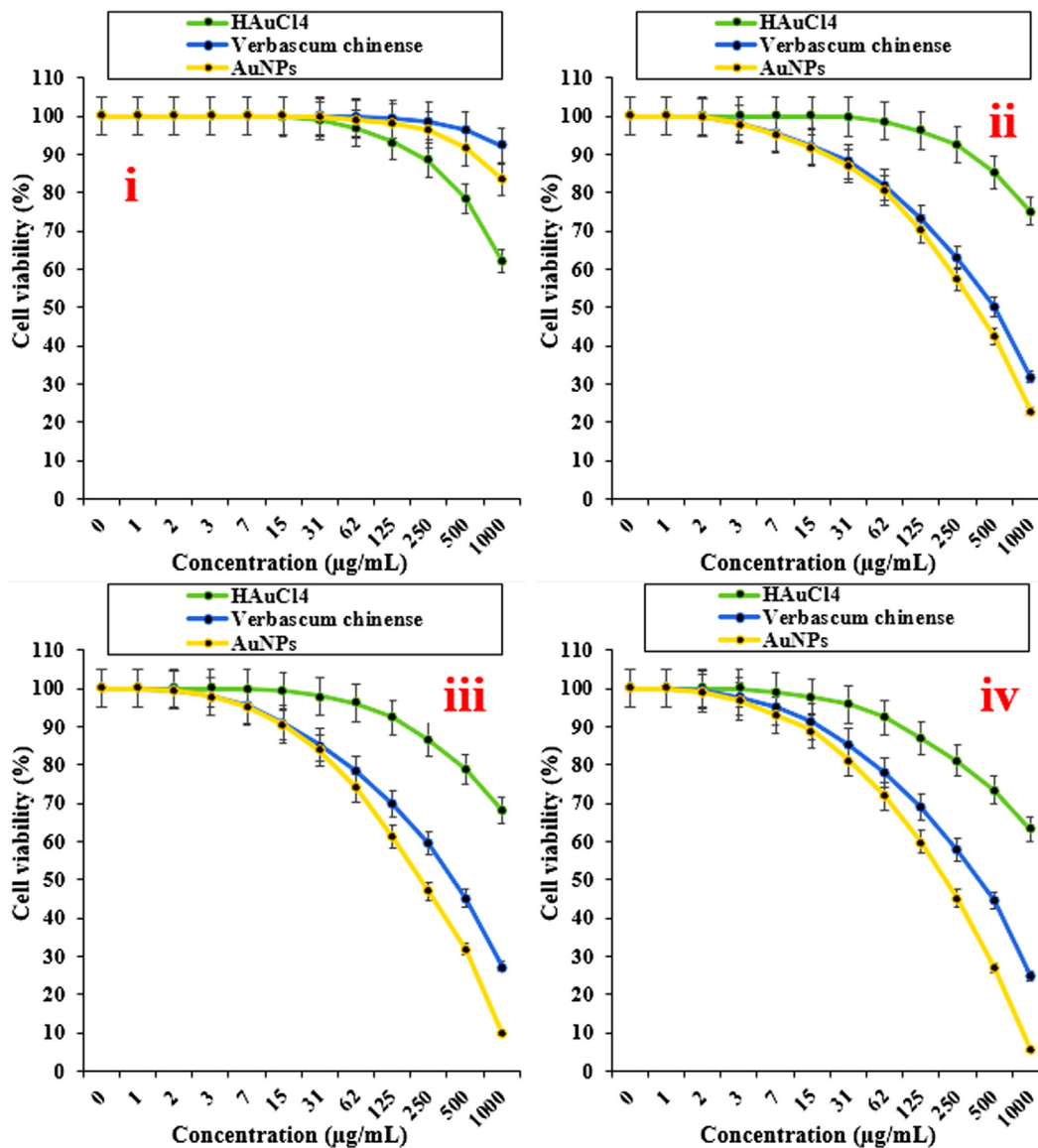


**Fig. 6** The anti-lung cancer properties of HAuCl<sub>4</sub>, *Verbascum chinense*, and AuNPs against normal (HUVEC (i)), well-differentiated bronchogenic adenocarcinoma (HLC-1 (ii)), moderately differentiated adenocarcinoma of the lung (LC-2/ad (iii)), and poorly differentiated adenocarcinoma of the lung (PC-14 (iv)) cell lines.

*3.6. Cytotoxicity and anti-human lung cancer potentials of gold nanoparticles synthesized using *Verbascum chinense**

Probably the anti-human lung cancer properties of gold nanoparticles against well-differentiated bronchogenic adenocarcinoma (HLC-1), moderately differentiated adenocarcinoma of the lung (LC-2/ad), and poorly differentiated adenocarcinoma of the lung (PC-14) are related to their antioxidant activities.

The previous researches have revealed that antioxidant compounds such as medicinal plants and gold nanoparticles as single electron donors can stabilize and scavenge the free radicals, which in conditions of oxidative stress may begin angiogenesis or carcinogenesis (Oganesvan et al., 1991; Radini et al., 2018). High levels of free radicals are observed in various cancerous cells and several accumulating evidences suggests that free radicals function as key signaling molecules stimulate different growth-related responses that finally begin tumorigenesis and

**Table 2** The IC<sub>50</sub> of HAuCl<sub>4</sub>, *Verbascum chinense*, and AuNPs in the anti-lung cancer test.

	HAuCl <sub>4</sub> (μg/mL)	<i>Verbascum chinense</i> (μg/mL)	AuNPs (μg/mL)
IC <sub>50</sub> against HUVEC	–	–	–
IC <sub>50</sub> against HLC-1	–	497	369
IC <sub>50</sub> against LC-2/ad	–	404	227
IC <sub>50</sub> against PC-14	–	399	210

angiogenesis (Oganesvan et al., 1991; Radini et al., 2018; Beheshtkhou et al., 2018). In detail, Free radical-induced development of cancer involves malignant transformation due to DNA mutations and changed gene expression through epigenetic mechanisms which in turn causes the uncontrolled proliferation of cancerous cells (Radini et al., 2018; Beheshtkhou et al., 2018). Many researchers reported a remarkable role of antioxidant compounds such as medicinal plants and gold nanoparticles in growth inhibition of prostate, ovary, breast, endometrial and lung, and colon cancer cells with removing free radicals (Sangami and Manu, 2017; Katata-Seru et al., 2018).

In the present experiment, the treated cells with several concentrations of the present HAuCl<sub>4</sub>, *Verbascum chinense*, and AuNPs were examined by MTT test for 48 h regarding the cytotoxicity properties on normal (HUVEC) and human lung cancer cell lines i.e., well-differentiated bronchogenic adenocarcinoma (HLC-1), moderately differentiated adenocarcinoma of the lung (LC-2/ad), and poorly differentiated adenocarcinoma of the lung (PC-14) (Fig. 6; Table 2). The absorbance rate was determined at 570 nm, which indicated extraordinary viability on normal cell line (HUVEC) even up to 1000 μg/mL for HAuCl<sub>4</sub>, *Verbascum chinense*, and AuNPs. In the case of human lung cancer cell lines, the viability of them reduced dose-dependently in the presence of HAuCl<sub>4</sub>, *Verbascum chinense*, and AuNPs. The IC<sub>50</sub> of *Verbascum chinense*, and AuNPs against HLC-1 cell line were 497 and 369 μg/mL, respectively; against LC-2/ad cell line were 404 and 227 μg/mL, respectively; and against PC-14 cell line were 399 and 210 μg/mL, respectively. The best result of anti-human lung cancer property of gold nanoparticles against the above cell lines was seen in the case of the poorly differentiated adenocarcinoma of the lung (PC-14) cell line.

#### 4. Conclusions

In the present study, *Verbascum chinense* L. leaf collected was applied for biosynthesizing gold nanoparticles as a safe and suitable material. After gold nanoparticles synthesizing, they were characterized by TEM, FE-SEM, UV Vis., and FT-IR. The above analyses revealed that gold nanoparticles were synthesized as the best possible form. In the FT-IR test, the presence of many antioxidant compounds with related bonds caused the excellent condition for reducing of gold in the gold nanoparticles, so that the antioxidant properties of gold nanoparticles were the better than the BHT as a positive control. Gold nanoparticles showed significant anti-human lung activities against well-differentiated bronchogenic adenocarci-

noma (HLC-1), moderately differentiated adenocarcinoma of the lung (LC-2/ad), and poorly differentiated adenocarcinoma of the lung (PC-14) cell lines. It looks these nanoparticles may be administrated as a chemotherapeutic drug for the treatment of several types of lung cancers especially well-differentiated bronchogenic adenocarcinoma, moderately differentiated adenocarcinoma of the lung, and poorly differentiated adenocarcinoma of the lung.

#### Funding

Project level: Mandatory project of Nantong Science and Technology Bureau (MS12020027), Topic: Indocyanine green near-infrared imaging in minimally invasive surgery for esophageal cancer.

#### Declaration of Competing Interest

The authors declare that they have no known competing financial interests or personal relationships that could have appeared to influence the work reported in this paper.

#### Acknowledgement

This project was supported by Researchers Supporting Project number (RSP-2021/230) King Saud University, Riyadh, Saudi Arabia.

#### References

- Cancer Research UK crukorg/cancerstats 2013.
- Jemal, A., Bray, F., Center, M.M., et al, 2011. Global cancer statistics. *A Cancer J. Clinicians CA* 61, 69–90.
- Centers for Disease Control and Prevention (US), 2004. The Health Consequences of Smoking: A Report of the Surgeon General Office of the Surgeon General (US); Office on Smoking and Health (US); Atlanta, GA.
- Rodriguez, E., Lilenbaum, R., 2010. Small cell lung cancer: past, present, and future. *Curr. Oncol. Rep.* 12, 327–334.
- Chang, A., 2011. Chemotherapy, chemoresistance and the changing treatment landscape for NSCLC Lung Cancer, 71, 3–10
- Zangeneh, A., Zangeneh, M.M., 2019. *Appl. Organometal. Chem.* 33., <https://doi.org/10.1002/aoc.5290> e5290.
- Hemmati, S., Joshani, Z., Zangeneh, A., Zangeneh, M.M., 2019. *Appl. Organometal. Chem.* 33., <https://doi.org/10.1002/aoc.5267> e5267.
- Ball, V., 2018. *Front. Bioeng. Biotechnol.* 6, 109.
- Sintubin, L., Windt, W.D., Dick, J., Mast, J., van der Ha, D., Verstraete, W., Boon, N., 2009. *Appl. Microbiol. Biotechnol.* 6, 741–749.
- Arunachalam, K.D., Annamalai, S.K., Hari, S., 2003. *Int. J. Nanomed.* 8, 1307–1315.
- Varma, R.S., 2012. *Curr. Opin. Chem. Eng.* 1, 123.
- Raut, R.W., Kolekar, N.S., Lakkakula, J.R., Mendhulkar, V.D., Kashid, S.B., 2010. *Nano-Micro Lett.* 2, 106.
- (a) Zangeneh, M.M., 2019. *Appl. Organometal. Chem.* 33 e5295. DOI:10.1002/aoc.5295. (b) Mohammadi, G., Zangeneh, M.M., Zangeneh, A., Siavosh Haghighi, Z.M., 2019. *Appl. Organometal. Chem.* 33 e5136. DOI:10.1002/aoc.5136.
- Zhaleh, M., Zangeneh, A., Goorani, S., Seydi, N., Zangeneh, M.M., Tahvilian, R., Pirabbasi, E., 2019. *Appl. Organometal. Chem.* 33, e5015.
- Shahriari, M., Hemmati, S., Zangeneh, A., Zangeneh, M.M., 2019. *Appl. Organometal. Chem.* 33., <https://doi.org/10.1002/aoc.5189> e5189.



- Zangeneh, M.M., Saneei, S., Zangeneh, A., Touthmalani, R., Haddadi, A., Almasi, M., Amiri-Paryan, A., 2019. *Appl. Organometal. Chem.* 33, <https://doi.org/10.1002/aoc.5216> e5216.
- Tveden-Nyborg, P., Bergmann, T.K., Lykkesfeldt, J., 2018. *Basic Clin. Pharmacol. Toxicol.* 123, 233–235.
- Riaza, M., Zia-Ul-Haqb, M., Jaafarc, H.Z.E., 2013. *Rev. Bras. Farmacogn.* 23, 948–959.
- Soni, A., Krishnamurthy, R., 2013. *Indian J. Plant Sci.* 2, 117–125.
- Peng, G., Tisch, U., Adams, O., Hakim, M., Shehada, N., Broza, Y. Y., Billan, S., Abdah-Bortnyak, R., Kuten, A., Haick, H., 2009. *Nat. Nanotechnol.* 4, 669–673.
- Singh, P., Pandit, S., Mokkaapati, V.R.S.S., Garg, A., Ravikumar, V., Mijakovic, I., 1979. *Int. J. Mol. Sci.* 2018, 19.
- Hosseinimehr, S.J., Mahmoudzadeh, A., Ahmadi, A., Ashrafi, S.A., Shafaghati, N., Hedayati, N., 2011. *Cancer Biother. Radiopharm.* 26, 325–329.
- Arulmozhi, V., Pandian, K., Mirunalini, S., 2013. *Colloids Surf. B Biointerfaces.* 110, 313–320.
- Mehwish, S., Islam, A., Ullah, I., Wakeel, A., Qasim, M., AliKhan, M., Ahmad, A., Ullah, N., 2019. *Biocat. Agri. Biotech.* 19, 101117.
- Kumar, R., Umar, A., Kumar, G., Nalwa, H.S., 2017. *Ceramics Inter.* 43, 3940–3961.
- Jin, S., Wu, C., Zhong Ye, Z., Ying, Y., 2019. *Sen. Act. B Chem.* 283, 18–34.
- van der Heijden, A.E.D.M., 2018. *Chem. Eng. J.* 350, 939–948.
- Shah, A.A., Hasan, F., Hameed, A., Ahmed, S., 2008. *Biotech. Adv.* 26, 246–265.
- Deshmukh, S.P., Patil, S.M., Mullani, S.B., Delekar, S.D., 2019. *Mat. Sci. Eng. C* 97, 954–965.
- Pereira, C., Pereira, A.M., Fernandes, C., Rocha, M., Mendes, R., Fernández-García, M.P., Guedes, A., Tavares, P.B., Grenèche, J. M., Araújo, J.P., Freire, C., 2012. *Chem. Mater.* 24, 1496–1504.
- Ramyadevi, J., Jeyasubramanian, K., Marikani, A., Rajakumar, G., Rahuman, A.A., 2012. *Mater. Lett.* 71, 114–116.
- Gultekin, D.D., Gungor, A.A., Onem, H., Babagil, A., Nadaroglu, H., 2016. *J Turk. Chem. Soc. A: Chem.* 3, 623–636.
- Rehana, D., Mahendiran, D., Kumar, R.S., Rahiman, A.K., 2017. *Biomed. Pharmacother.* 89, 1067–1077.
- Del Mar Delgado-Povedano, M., De Medina, V.S., Bautista, J., Priego-Capote, F., De Castro, M.D., 2016. *J. Function Foods.* 24, 403–419.
- Jeong, S.C., Koyyalamudi, S.R., Jeong, Y.T., Song, C.H., Pang, G., 2012. *J. Med. Food.* 1, 58–65.
- Sankar, R., Maheswari, R., Karthik, S., Shivashangari, K.S., Ravikumar, V., 2014. *Mat. Sci. Eng. C.* 44, 234–239.
- Namvar, F., Rahman, H.S., Mohamad, R., Baharara, J., Mahdavi, M., Amini, E., Chartrand, M.S., Yeap, S.K., 2014. *Int. J. Nanomed.* 19, 2479–2488.
- Oganesvan, G., Galstyan, A., Mnatsakanyan, V., Paronikyan, R., Ter-Zakharyan, Y.Z., 1991. *Chem. Nat.* 27, 247.
- Radini, I.A., Hasan, N., Malik, M.A., Khan, Z., 2018. *J. Photochem. Photobiol. B.* 183, 154–163.
- Beheshtkhoo, N., Kouhbanani, M.A.J., Savardashtaki, A., Amani, A. M., Taghizadeh, S., 2018. *Appl. Phys. A.* 124, 363–369.
- Sangami, S., Manu, B., 2017. *Environ. Technol. Innov.* 8, 150–163.
- Katata-Seru, L., Moremedi, T., Aremu, O.S., Bahadur, I., 2018. *J. Mol. Liq.* 256, 296–304.